# Laminar Flows in Tubes with Step Changes in Cross Section

**F. W. SCHMIDT and K. WIMMER**

**Department of Chemical Engineering**
**Pennsylvania State University, University Park, Pennsylvania 16802**

A considerable amount of attention has been given to the calculation of the velocity profiles and the evaluation of the pressure drop in the entrance region of a straight duct with laminar flow. A majority of the methods of calculation employ the boundary-layer assumptions, thus neglecting the axial transport of vorticity and assuming that the pressure is a function of axial distance only. More recently these items have been taken into consideration and solutions have been obtained by use of the momentum equations and finite-difference methods. A comparison of the various methods for a straight tube and a parallel-plate channel has been presented by Schmidt and Zeldin (*1*). In all these studies the condition of the flow at the tube inlet was considered to be irrotational with the fluid having a uniform axial velocity. When the complete set of Navier-Stokes equations was used, $r$- and $z$-directional momentum equations, the solutions showed a Reynolds number dependency. For moderate and high Reynolds numbers, the irrotational uniform velocity assumption is a generally accepted approximation for the conditions produced by a sudden contraction into a well-rounded entrance. As the Reynolds number decreases or the change in cross section at the entrance to the tube becomes more abrupt the flow at the tube inlet deviates considerably from these entrance conditions and it becomes dependent upon the flow configuration upstream. The authors are not aware of any published results for laminar flow in a tube with a step change in cross section.

The velocity profiles and pressure drop in a straight tube with an abrupt change in cross section have been studied. The change in section occurred at $Z = 0$. The tube was extended to plus and minus infinity with fully developed velocity profiles being assumed at these locations. A sketch of the section is shown in Figure 1 where the larger tube had a radius twice that of the smaller tube.

The flow is described by the continuity and the $r$- and $z$-directional momentum equations. The equations were nondimensionalized and the stream function and vorticity were introduced to reduce the number of equations and eliminate the pressure terms. The resulting set of elliptic equations was solved using finite-difference techniques. An axial transformation of the following form was used:

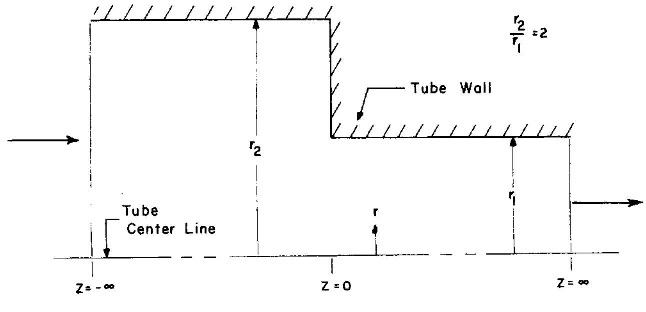


**Fig. 1. Tube configuration.**

$$S = 1 - \frac{1}{1 + CZ} \quad \text{for } 0 < Z < \infty$$
$$S = -\left[1 - \frac{1}{1 - CZ}\right] \quad \text{for } -\infty < Z < 0 \qquad (1)$$

where $C$ is an arbitrary positive constant introduced in order to obtain a smaller grid pattern in the axial direction near the change in cross section. The spacial domain was subdivided into a system of 40 equal subdivisions in the S domain.

A logarithmic transformation was used in the radial direction with 40 radial subdivisions in the larger tube and 20 radial subdivisions in the smaller. The transformation was selected to yield finer grid spacing at $r_1$ and a coarser spacing in the vicinity of the center line and the wall of the larger tube. Allen's method was used in the formation of the finite-difference equations. The resulting set of algebraic equations was solved using a successive over-relaxation technique. A complete discussion of the solution technique was presented by Wimmer (*2*).

Computations were made with Reynolds numbers of 50, 100, 1,000 and 10,000, based upon the larger tube

TABLE 1. GRID LOCATIONS

| Node column | Z+ |
|---|---|
| 1 | $-\infty$ |
| 17 | $-0.00132$ |
| 19 | $-0.00058$ |
| 21 | 0 |
| 23 | 0.00058 |
| 25 | 0.00132 |
| 27 | 0.00226 |
| 29 | 0.00351 |
| 31 | 0.00526 |
| 41 | $\infty$ |

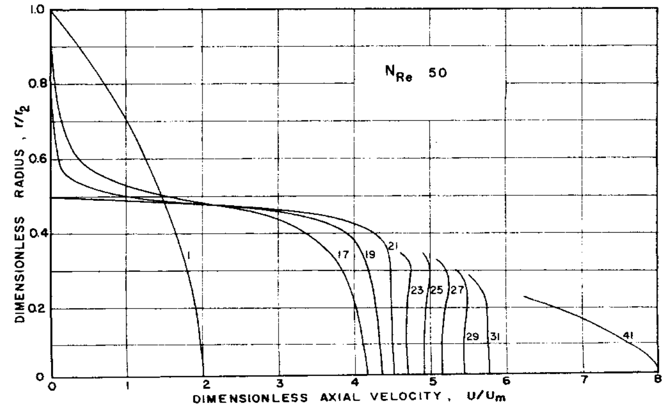


**Fig. 2. Axial velocity profiles.**

diameter. As we mentioned, the majority of previous studies have incorporated the boundary-layer assumptions. These assumptions are valid only for high Reynolds number flows. The results for a Reynolds number of 10,000 are presented in this note solely for the purpose of presenting a solution which would approach that obtained by making the boundary-layer assumptions.

## VELOCITY

The axial velocity profiles at several locations are shown in Figure 2. The numbers next to the curves indicate the nodal column number, and the nondimensional axial location at these locations may be found using Table 1. A central concavity in the velocity profiles either at or shortly downstream from the small diameter tube entrance was noted for the three lower Reynolds number flows. The concavity decreased as the Reynolds number increased and was not observed at $N_{Re} = 10{,}000$. At Reynolds numbers of 50 and 100 a small area of flow recirculation was observed in the corner formed by the intersection of the vertical wall at $Z = 0$ and the wall of the large tube. As the Reynolds number was increased the recirculation disappeared. In all cases investigated the axial velocity at the small tube entrance deviated greatly from that of a uniform profile. The development of the center line axial velocity is shown in Figure 3. At low Reynolds number the effect of the change in section is propagated upstream into the large diameter tube.

## PRESSURE DROP

The total pressure drop in the tube is expressed as the

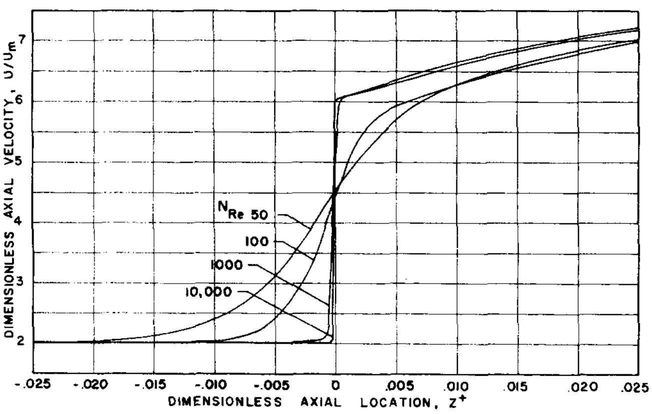


**Fig. 3. Center line axial velocity development.**

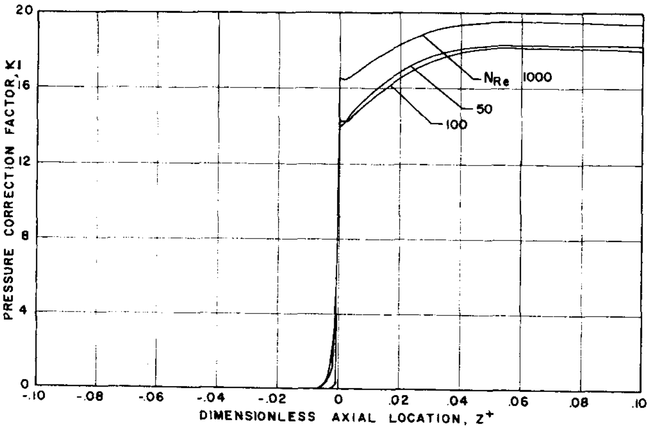


***Fig. 4. Pressure correction factor.***

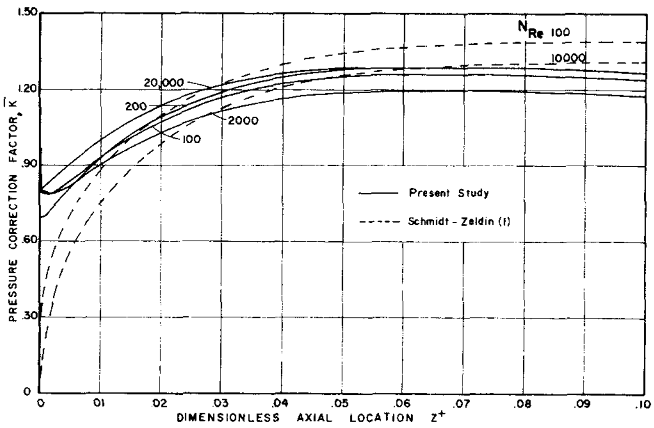


**Fig. 5. Small tube section pressure correction factor.**

sum of the pressure drop which would occur if the flow were fully developed over the entire axial interval $\bar{\phi}_f$, plus a correction factor to account for the change in flow caused by the reduction in tube radius $K$. The total pressure drop is

$$\frac{\overline{P}|_{Z+=-0.1} - \overline{P}|_{Z+}}{\frac{\rho u_m^2}{2}} = \bar{\phi}_f + K$$

The variation in $K$ with axial location is shown in Figure 4. It is readily seen that the pressure drop required to overcome the viscous forces on the fluid and increase the inertia of the fluid is felt upstream of the location where the change in cross section occurs. As the Reynolds number is increased, the value of $K$ immediately inside the small tube entrance peaks, then decreases slightly before increasing to a maximum value. Because of the characteristics of the flow, the inertial forces, both the axial and radial, increase greatly at the small tube entrance. As the flow moves downstream, the radial inertial forces decrease, resulting in the slight decrease in total pressure drop. As one moves further downstream the pressure drop increases as viscous forces become more dominant.

In order to compare the pressure drop results of this study with those previously noted (*1*), another pressure drop correction factor is presented:

$$\frac{P_0 - \overline{P}|_{Z+}}{\frac{\rho u^2_{ms}}{2}} = \frac{64}{N_{Re}^1} Z + \overline{K}$$

where the reference pressure $P_0$ is that at the center line at axial location $Z+ = 0$ and the mean velocity and Reynolds number are based upon the small tube. None of the flow configurations in this study had zero or even low vorticity values at the entrance to the small tube. These correction factors together with those previously reported are shown in Figure 5. As can be seen from this figure the values of $\overline{K}$ from the present study are initially higher than those obtained using the entrance conditions of uniform velocity and zero vorticity. As one moves downstream this trend is reversed.

## NOTATION

$C$ = transformation constant
$N_{Re}^1$ = Reynolds number bases on small tube
$N_{Re}$ = Reynolds number, $2r_2\, u_m/\nu$
$P$ = pressure
$\overline{P}$ = area integrated average pressure

$r$ = radius
$r_1$ = radius of smaller tube
$r_2$ = radius of larger tube
S = transformal axial length
$u$ = velocity
$u_m$ = mean velocity in large tube
$u_{ms}$ = mean velocity in small tube
$z$ = axial distance
Z = nondimensional axial length $z/r_2$
$Z_+$ = $Z/N_{Re}$

**Greek Letters**

$\rho$ = density
$\nu$ = kinematic viscosity

#### LITERATURE CITED


1. Schmidt F. W., and B. Zeldin, *AIChE J.*, 15, 612 (1969).
2. Wimmer, K., M.S. thesis, Pennsylvania State Univ. (1970).


# Application of Quasilinearization to Countercurrent CSTR'S


**SALVATORE J. CASAMASSIMA and EDWARD N. ZIEGLER**

**Department of Chemical Engineering**
**Polytechnic Institute of Brooklyn, 333 Jay Street, Brooklyn, New York 11201**


Stagewise process problems commonly encountered in engineering design include the analysis of extractors, distillation towers, and reactor cascades. Solutions to these kinds of problems which may be resolved into linear equations have been established by either analytical or graphical techniques. By assuming a constant equilibrium or distribution coefficient or by assuming first order reaction, the equations become linear permitting the use of these standard techniques. If, however, the true nature of the equilibrium and/or rate expressions is known, it may be far more accurate to use the more rigorous system equations, although they may be nonlinear. The most popular method for handling stagewise nonlinear processes is that of linearizing the equations of the process matrix by the Newton-Raphson method. The current work is concerned with applying a relatively new technique, quasilinearization developed by Bellman and Kalaba (*1*), to the finite difference equations of stagewise reaction processes.

#### PURPOSE OF STUDY

A recent paper by Kowalczyk (*2*) shows that both the methods of solution and the analytical results obtained in applying finite difference calculus to a series of CSTR's are analogous to the solution of differential equations that are encountered in plug flow reactors. It is the intention of this communication to apply the method of quasilinearization to the nonlinear finite difference equations of cascaded CSTR's with boundary conditions at different stages (split conditions). Let it be known that this is simply an attempt to solve these difference equations by quasilinearization and not a theoretical proof of its validity or lack of validity for this application. The numerical method of quasilinearization which has been chosen has two major advantages. First of all, nonlinear equations using this technique converge rapidly to solutions (i.e., quadratic convergence). Secondly, solutions can be obtained even with very poor starting values of unknown initial conditions. Lee (*3*) and Lee and Noh (*5*) have shown that quasilinearization is a very powerful technique in solving nonlinear differential and difference equations occurring in chemical engineering (e.g., tubular reactor and distillation column).

Consider the following problem of a series of continuous stirred-tank reactors whose effluents and feed streams are flowing countercurrently (Figure 1). A steady material balance on reactor $n + 1$ for each component is made.

$$0 = QC_{An} + QC_{An+2} - 2QC_{An+1} - kC_{An+1}C_{Bn+1}V_R \quad \text{for } A \qquad (1)$$

$$0 = QC_{Bn} + QC_{Bn+2} - 2QC_{Bn+1} - kC_{An+1}C_{Bn+1}V_R \quad \text{for } B \qquad (2)$$

The generation rate equation used is

$$r_{An+1} = -kC_{An+1}C_{Bn+1}, \text{ i.e., } (A + B \rightarrow \text{products}).$$

Note that this term is nonlinear with respect to concentration $C_{An+1}$ because $C_{Bn+1}$ is also dependent on the concentration $A$.

The dimensionless variables introduced are

$$Y_{An+1} = C_{An+1}/C_{A0}, \quad Y_{Bn+1} = C_{Bn+1}/C_{A0},$$

$$X = kC_{A0} \; V_R/Q$$

The material balance for constant $X$ reduces to difference equations

$$0 = Y_{An} + Y_{An+2} - 2Y_{An+1} - X\, Y_{An+1}\, Y_{Bn+1} \qquad (3)$$

$$0 = Y_{Bn} + Y_{Bn+2} - 2Y_{Bn+1} - X\, Y_{An+1}\, Y_{Bn+1} \qquad (4)$$

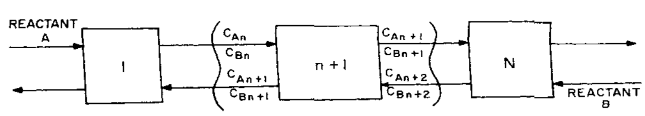


**Fig. 1. Flow diagram of stage of countercurrent CSTR cascade.**

Correspondence concerning this communication should be addressed to Professor Edward N. Ziegler.